GeCat 2014: Advances and prospects in heterogeneous catalysis

Catalyst optimization for enhanced propylene formation in the methanol-to-olefins reaction

Pit Losch [a], Marilyne Boltz [a], Benoît Louis [a,*], Sachin Chavan [b], Unni Olsbye [b]

[a] Laboratoire de synthèse réactivité organiques et catalyse, Institut de Chimie, Université de Strasbourg, UMR 7177 CNRS, 4, rue Blaise-Pascal, 67000 Strasbourg cedex, France
[b] inGAP Center of Research Based Innovation, Department of Chemistry, University of Oslo, P.O. Box 1033, Blindern, 0315 Oslo, Norway

ARTICLE INFO

ABSTRACT

ZSM-5 zeolites possessing different chemical compositions, acidities and crystal sizes, were synthesized and characterized by XRD, SEM and FTIR. Those as-prepared acid catalysts were tested in the conversion of methanol into light olefins at 673 K under atmospheric pressure. Propylene-to-ethylene ratios above 5 were achieved over ZSM-5 zeolite catalyst prepared via the fluoride route. This promising methanol-to-propylene (MTP) catalyst was designed both at the molecular scale, *exhibiting low Brønsted acid site density*, and at the microscopic level since *large crystals (25 μm) with few defects* were obtained. Aiming in a possible industrial application, the synthesis medium has to be seriously modified, thus avoiding harmful hydrofluoric acid use. Hydrochloric and phosphoric acids were therefore chosen as alternatives and resulted in the same ZSM-5 crystal morphologies and similar catalytic performance.

© 2014 Académie des sciences. Published by Elsevier Masson SAS. All rights reserved.

RÉSUMÉ

De nos jours, les procédés de conversion du méthanol en oléfines légères (MTO) et plus particulièrement du méthanol en propylène (MTP) sont considérés comme des voies attractives et viables pour la valorisation des ressources en gaz naturel. Notre stratégie est de développer un catalyseur zéolithique de type ZSM-5, *via la synthèse en milieu fluorure*, ayant des propriétés désirées pour la réaction MTP effectuée à 400 °C. Un catalyseur présentant une densité de sites acides faible et une taille de cristal de 25 μm a démontré des performances intéressantes. De plus, nous avons été en mesure de substituer l'acide fluorhydrique par de l'acide phosphorique dans le gel de synthèse et ainsi développer une voie plus écocompatible pour le design du catalyseur.

© 2014 Académie des sciences. Publié par Elsevier Masson SAS. Tous droits réservés.

1. Introduction

The transformation of methanol to hydrocarbons (MTH) to produce high-octane gasoline [1] represents a valuable process involving zeolite or zeotype catalysts, which received considerable industrial interest [2–5]. Besides the Mobil Oil methanol-to-gasoline (MTG) process, Lurgi's methanol-to-propene (MTP) [6], Norsk Hydro/UOP's methanol-to-olefins (MTO) and Haldor Topsøe TIGAS processes [7] are also commercialized [8,9].

The MTO reaction is a competitive option for the valorization of stranded gas reserves. Several studies

* Corresponding author.
E-mail address: blouis@unistra.fr (B. Louis).

devoted either to the reaction mechanism or to the technology were therefore undertaken [9–17]. In addition, the worldwide market demand in ethylene and propylene is gradually raising and projected growth rates in coming decades are further expected to remain high [18]. ZSM-5 zeolite catalysts are often employed and several strategies targeting to achieve an improved selectivity toward light olefins have been tempted: operating conditions, change in reactor configuration [19], proper tailoring of catalyst Brønsted acidity [20], development of structured catalyst [12,21].

We have recently investigated the influence of both Brønsted acid sites density and crystal size on activity/selectivity in the MTO reaction [22]. The main goal was to raise and then maintain a high selectivity toward propylene, hence to develop a simple strategy for designing a MTP catalyst with the MFI structure. With these promising results in hand, it was decided to further optimize ZSM-5 zeolites synthesized under fluoride conditions. Indeed, hydrofluoric acid has to be replaced to warrant industrial catalyst implementation. This study will therefore focus on the design of a novel MTP-catalyst generation, synthesized in the absence of HF.

2. Experimental

2.1. Catalyst preparation

Several ZSM-5 zeolites were synthesized via fluoride-mediated syntheses to investigate different parameters: density of Brønsted acid sites, crystal size, chemical composition. One ZSM-5 zeolite prepared via the classical alkaline route was used as the reference material and named MFI-R [22]. MFI-F catalyst was prepared via the fluoride-mediated route according to our previous studies [23]. The same procedure was followed while substituting hydrofluoric acid by either hydrochloric acid or phosphoric acid to maintain a neutral pH (Table 1). These samples were named MFI-FCl and MFI-FP, respectively. All ZSM-5 samples obtained in either NH_4- or Na-form were either ion-exchanged and calcined or simply calcined. Cationic exchange was repeated three times, using 20 mL of a 1.0 M aqueous NH_4NO_3 solution per gram of catalyst. The solution was kept at 348 K for 2 h before catalyst separation by centrifugation. The solid was dried overnight

in an oven at 373 K and further calcined in static air during 6 h at 823 K.

2.2. Characterization

Specific surface areas (SSA) of the materials were determined by N_2 adsorption-desorption measurements performed at 77 K employing the BET-method (Micromeritics sorptometer Tri Star 3000). X-ray diffraction (XRD) patterns were recorded on a Bruker D8 Advance diffractometer, with a Ni detector side filtered Cu Kα radiation (1.5406 Å) over a 2θ range of 5° to 60°. Scanning electron microscopy (SEM) micrographs were acquired on a JEOL FEG 6700F microscope working at a 9 kV accelerating voltage. The Si/Al ratios of the materials were determined by EDX analysis coupled with the SEM chamber.

Infrared spectroscopy (FTIR) spectra were recorded in controlled atmosphere at 2 cm^{-1} resolution on a Bruker Vertex 80 FTIR spectrophotometer, equipped with a MCT detector and using a homemade IR cell. FTIR spectra were collected in transmission mode on a thin film prepared by deposition of a zeolite water suspension on a silicon wafer. The difference in the Brønsted acid strength of these samples was derived from CO adsorption. In order to compare the IR band intensities, spectra were normalized to the overtone mode at 2005 cm^{-1}.

2.3. MTO reaction

Prior to use, the catalysts were activated at 823 K with a gradient of 15 K/min in static air. The zeolites were sieved and particles < 250 μm were used in the following experiments. Sixty milligrams of zeolite were introduced in a tubular quartz reactor and packed between quartz wool plugs. A constant nitrogen flow, of 20 mL/min was flown through a methanol saturator, cooled at 273 K, to achieve a WHSV = 1.12 g_{MeOH}/g_{cat} * 1/h. The reactant was subsequently fed to the reactor containing the catalyst at 673 K. GC analysis was performed on a HP GC5890 equipped with a 50-m capillary column (PONA) and a flame ionization detector (FID). The activity of the catalysts was expressed in terms of methanol and dimethylether conversion, calculated from the difference between inlet and outlet concentrations of methanol (DME is considered as an intermediate). The selectivity was defined as the mole ratio of each product referred to the moles of

Table 1
Textural properties and catalytic performances of as-prepared catalysts.

Entry	Catalyst	pH-gel	Si/Al/(P)-gel	MeOH conversion[a] [%[	S_{C2}[b] [%]	S_{C3}[b] [%[	S_{C2-C4}[b] [%[
1	H-ZSM-5R	10	25	14	15	27	56
2	H-ZSM-5F	6–7	67	98	7	36	66
3	H-ZSM-5FCl	6–7	100	64	26	35	78
4	H-ZSM-5FP	6–7	100/1/11	0	–	–	–
5	H-ZSM-5FP	7	100/1/1	13	33	35	83
6	H-ZSM-5FP	7	100/3/2	54	32	33	78

[a] After 48 h on stream.
[b] After 15 min on stream at complete methanol conversion.

converted methanol and dimethylether. Eqs. (1) and (2) were used to calculate the (1) conversion, (2) the respective selectivity and (3) the C_3/C_2 ratio:

$$X = \frac{N\ MeOH\ In - (N\ MeOH\ Out + 2*N\ DME)}{N\ MeOH\ In} *100\% \tag{1}$$

$$S = \frac{(\Sigma)\alpha*N(CH_2)}{N\ MeOH\ In - (N\ MeOH\ Out + 2*N\ DME)} *100\% \tag{2}$$

where α represents the number of C-atoms in the considered product, (Σ) applied for the calculation of the selectivity towards light olefins C_2–C_4 fraction. In addition, the denominator corresponds to consumed methanol and dimethylether (being considered as a reactant).

$$C_3/C_2 = \frac{N(C3H6)}{N(C2H4)} \tag{3}$$

3. Results

3.1. Characterization of the catalysts

XRD patterns of all as-prepared zeolites exhibited the sole MFI structure. Fig. 1 shows the pattern of the MFI-F sample.

SEM analysis was performed to evaluate the crystal morphologies and determine the Si/Al ratios of the different catalysts (EDX analysis). MFI-R exhibited the classical coffin-shape morphology, along with a crystal size of 5 μm. The MFI-F material prepared via fluoride-mediated route led to the formation of giant prismatic crystals having ∼15–20 μm in size (Fig. 2a). This material exhibits a very high cristallinity (Figs. 1 and 2a). The two samples synthesized in the absence of HF, MFI-FP (Fig. 2b) and MFI-FCl (Fig. 2c) also exhibit large prismatic crystals ∼20–30 μm, along with the presence of amorphous material.

Table 1 presents the Si/Al ratio and the pH of the syntheses as well as reactivity data. The specific surface areas were comprised for all zeolites between 305 and 348 m²/g in line with values usually observed for MFI-type zeolites.
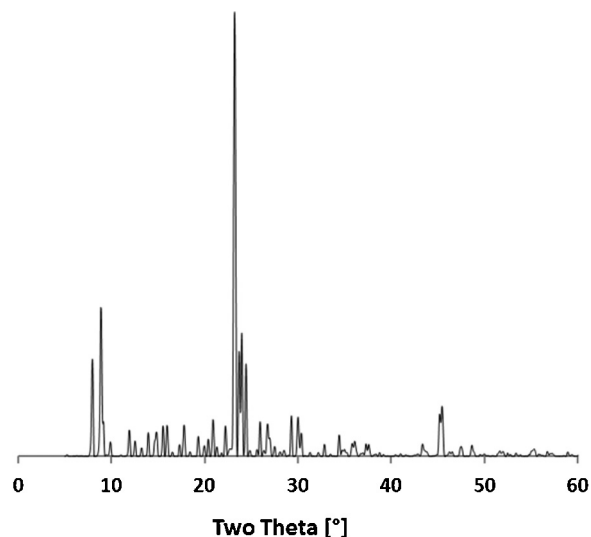
Fig. 1. X-ray diffraction pattern of MFI-F zeolite.

A three-time higher density of BrØnsted acid sites was measured by H/D exchange technique [24,25] over MFI-R when compared with MFI-F zeolite, *i.e; 1.00 and 0.31 mmol H^+/g*, respectively [22]. This result is in agreement with a higher Si/Al ratio observed for MFI-F samples (Table 1). Fig. 3 presents the IR spectra of MFI-F zeolite measured during interaction with CO at 77 K. The peak attributed to the Brønsted acid sites (3610 cm^{-1}) was red shifted to 3305 cm^{-1} for MFI-F and MFI-R samples upon interaction with CO, thus indicating similar acid strength. The weak signal at 3750 cm^{-1} indicates that only few defects (silanols) are present in MFI-F sample. When considering the ν(C–O) region (2050–2250 cm^{-1}), the main peak observed at 2174 cm^{-1} is attributed to an interaction with the Si–OH–Al bridging sites. Furthermore, a significant vibration centered at 2169 cm^{-1}, attributed to CO interaction with extra-framework Al (EFAl) sites, was also observed.

3.2. Methanol-to-olefins reaction

Whereas a continuous and drastic decrease in methanol conversion was observed over MFI-R reference catalyst, MFI-F catalyst exhibited a high stability with time on stream
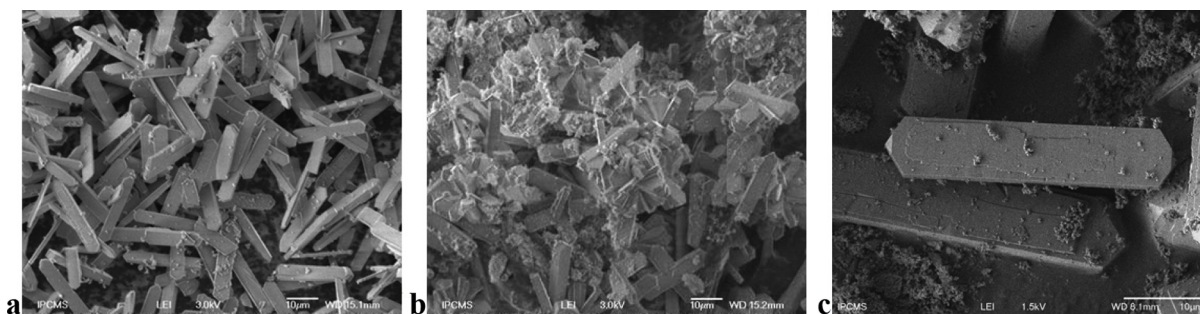
Fig. 2. Scanning electron microscopy images of fluoride-mediated materials: a: MFI-F zeolites synthesized in pure fluoride medium; b: MFI-FP in the presence of phosphoric acid; c: MFI-FCl in the presence of hydrochloric acid.
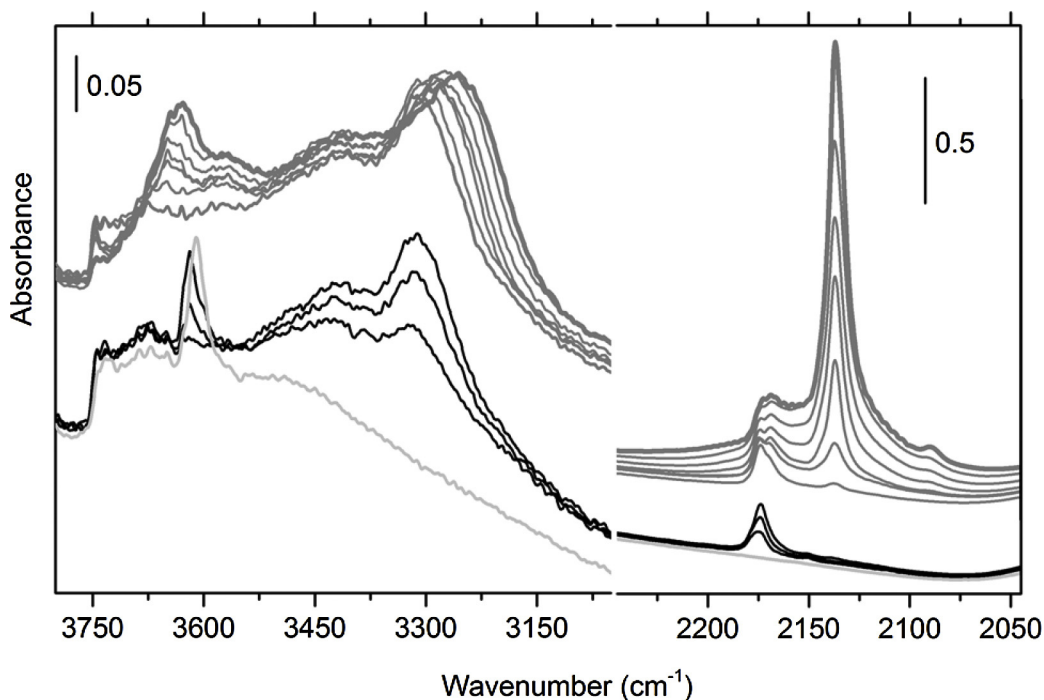
Fig. 3. Infrared spectroscopy (FTIR) spectrum of MFI-F pretreated at 873 K for 1 h, following CO adsorption at 77 K. **Left panel**: the ν(OH) region; **right panel**: the ν(CO) region. The CO coverage decreases successively from bold gray curve to light gray curve in the spectrum.

[22]. Indeed, the initial methanol full conversion diminished to 20% after 48 h on stream for MFI-R zeolite (Table 1). Besides, only minor changes in product selectivities were observed during the course of the reaction. The propylene-to-ethylene ratio was maintained between 2 and 2.5. In contrast, MFI-F catalyst preserved a complete methanol conversion during the whole test along with the same selectivities toward the reaction products (Table 1).

A high propylene-to-ethylene ratio $C_3/C_2 = 5.5$ was achieved and kept constant during 48 h on stream. The global selectivity in propylene was nearly 40%, being thus the major product obtained (Table 1). We have therefore decided to vary the weight hourly space velocity (WHSV) in order to further improve the $C_{3=}/C_{2=}$ ratio for this catalyst. Fig. 4 presents the methanol conversion and the $C_{3=}/C_{2=}$ ratio as a function of MFI-F catalyst weight at constant gas feed.

In parallel to a decrease in methanol conversion, it is worthy to note that a six-time raise in the WHSV led to a further enhancement of the propylene-to-ethylene ratio up to 8, *albeit* at the expense of methanol conversion. The global selectivity in propylene was kept constant at 41%. The major difference between this catalyst (prepared in

Fig. 4. Methanol conversion and propylene/ethylene ratio as a function of weight hourly space velocity for MFI-F catalyst (numbers indicate the propylene/ethylene ratio).
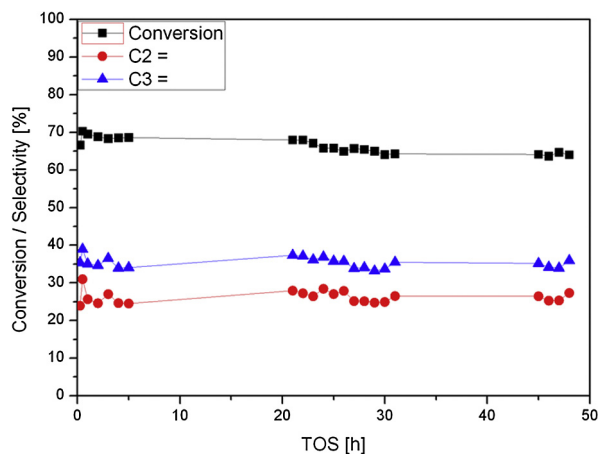
Fig. 5. Conversion and selectivities toward ethylene and propylene for MFI-FCl catalyst.
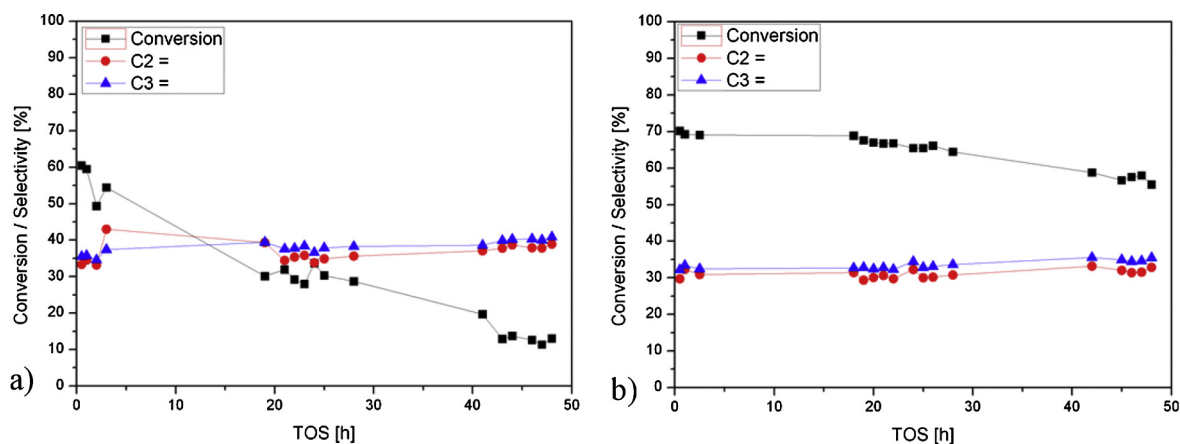
Fig. 6. Conversion and selectivities toward ethylene and propylene for two different MFI-FP-catalysts: a: same Si/Al ratio than MFI-F catalyst; b: higher Al content.

neutral medium) and the reference catalyst relies on its lower density of Brønsted acid sites. Indeed, less sites are present within these rather giant crystals, thus raising the dispersion of the active sites.

After thorough investigations of promising MFI-F catalyst, we have decided to improve the synthesis methodology by avoiding hydrofluoric acid use. The strategy was to test conventional hydrochloric acid on the one hand and phosphoric acid on the other hand to see whether P may have or not an influence on the catalyst performance, as already mentioned by Hua et al. [20].

Figs. 5 and 6 present the catalytic profiles, methanol conversion and selectivity to light olefins for MFI-FCl and MFI-FP zeolites.

As already seen in Table 1, MFI-FCl zeolite allows achieving the same selectivity toward propylene as MFI-F catalyst. In contrast, the propylene-to-ethylene ratio remains rather low at ~ 1.3. MFI-FCl catalyst remained active during two days on stream (at least). The single substitution of hydrofluoric acid did not drastically alter the catalyst's properties.

Regarding the substitution by phosphoric acid (neutral), a non-competitive MTO-catalyst was produced. Indeed, a continuous and drastic loss in methanol conversion was observed (Fig. 6a). However, by properly tailoring Si/Al/P elemental composition, a competitive catalyst could be prepared (Entry 6, Table 1). This P-containing MFI zeolite exhibited a very slow deactivation and high ethylene selectivity (32%) with a propylene-to-ethylene ratio = 1. It is therefore worthy to mention that the modulation of P/Al/Si in the gel for preparing ZSM-5 zeolites is a critical parameter to design a powerful MTO-catalyst. XRF elemental analysis of the latter H-ZSM-5FP confirmed the presence of P in the zeolite after calcination, i.e. P/Al = 0.24. Whereas no chlorine could be detected after MFI-FCl calcination, nearly one P-atom is present per 4 Al-atoms in more stable H-ZSM-5FP zeolite for the MTO reaction.

To summarize, it is therefore possible to avoid HF use for preparing valuable MTO-catalysts using less harmful HCl or H_3PO_4 acids.

Besides environmental concerns, a proper combination of Si/Al/P elements in the precursor gel is necessary to achieve a high stability and to maintain a high selectivity toward C_2–C_4 olefins. Further studies are under progress to evaluate the possible neutralization of acid sites by integration of phosphate tetrahedra within the zeolite framework. Furthermore, this generation of P-catalyst exhibits a high ethylene selectivity, which in turn supports the hypothesis of phosphate integration in the porous network, thus leading to higher steric constraints [20]. Likewise silicoaluminophosphates [26], a possible insertion of phosphate in MFI zeolite crystalline structure could lead to a different behaviour in acid-catalyzed reactions. Hence, MFI-FP type catalysts will be further investigated to see whether P-atoms are integrated or not in the framework by solid-state ^{31}P MAS NMR and EXAFS studies.

4. Conclusion

A novel generation of promising MTO-catalysts was successfully developed by adapting the ZSM-5 zeolite preparation procedure, along with tailored Brønsted acidity and crystal size.

High propylene-to-ethylene ratios (> 5) were achieved over a ZSM-5 zeolite prepared via the fluoride route. Consequently, it was tried to render the synthesis in fluoride medium more environmentally friendly. The different zeolites obtained exhibited interesting MTO-features, such as high stability when prepared with hydrochloric acid, or high ethylene selectivity for those prepared with phosphoric acid.

Finally, the latter catalysts are probably affected by the presence of phosphorous in the zeolite framework, which may alter the acid-base properties of ZSM-5 zeolite.

References

[1] C.D. Chang, Catal. Rev. Sci. Eng. 25 (1983) 1.
[2] S. Kvisle, T. Fuglerud, S. Kolboe, U. Olsbye, K.P. Lillerud, B.V. Vora, in: H. Ertl, H. Knözinger, F. Schüth, J. Weitkamp (Eds.), Handbook of Heterogeneous Catalysis, 6, Wiley-VCH, Weinheim, 2008 pp. 2950–2965.
[3] F.J. Keil, Microporous Mesoporous Mater. 29 (1999) 49.
[4] M. Stöcker, Microporous Mesoporous Mater. 29 (1999) 3.
[5] P. Barger, in: M. Guisnet, J.P. Gilson (Eds.), Zeolites for Cleaner Technologies. Catalytic Science Series (vol 3), Imperial College Press, 2002, pp. 239–260.
[6] H. Koempel, W. Liebner, Stud. Surf. Sci. Catal. 167 (2007) 261.
[7] J.Q. Chen, A. Bozzano, B. Glover, T. Fuglerud, S. Kvisle, Catal. Today 106 (2005) 103.
[8] M. Boltz, P. Losch, B. Louis, Adv. Chem. Lett. 1 (2013) 247.
[9] U. Olsbye, S. Svelle, M. Bjørgen, P. Beato, T.V.W. Janssens, F. Joensen, S. Bordiga, K.P. Lillerud, Angew. Chem. Int. Ed. 51 (2012) 5810.
[10] A.G. Gayubo, A.T. Aguayo, M. Olazar, R. Vivanco, J. Bilbao, Chem. Eng. Sci. 58 (2003) 5239.
[11] J.F. Haw, W. Song, D.M. Marcus, J.B. Nicholas, Acc. Chem. Res. 36 (2003) 317.
[12] F.C. Patcas, J. Catal. 231 (2005) 194.
[13] I. Štich, J.D. Gale, K. Terakura, M.C. Payne, J. Am. Chem. Soc. 121 (1999) 3292.
[14] H.A. Zaidi, K.K. Pant, Catal. Today 96 (2004) 155.
[15] M. Bjørgen, U. Olsbye, S. Kolboe, J. Catal. 215 (2003) 30.
[16] S. Ivanova, C. Lebrun, E. Vanhaecke, C. Pham–Huu, B. Louis, J. Catal. 265 (2009) 1.
[17] T.Y. Park, G.F. Froment, Ind. Eng. Chem. Res. 40 (2001) 4172.
[18] G.A. Olah, A. Goeppert, G.K.S. Prakash, Beyond Oil and Gas: The Methanol Economy, Wiley-VCH, Weinheim, 2006.
[19] K.P. Moller, W. Bohringer, A.E. Schnitzler, E. van Stehen, C.T. O'Connor, Microporous Mesoporous Mater. 29 (1999) 127–144.
[20] J. Liu, C.X. Zhang, Z.H. Shen, W. Hua, Y. Tang, W. Shen, Y.H. Yue, H.L. Xu, Catal. Commun. 10 (2009) 1506.
[21] S. Ivanova, B. Louis, B. Madani, J.P. Tessonnier, M.J. Ledoux, C. Pham-Huu, J. Phys. Chem. C 111 (2007) 4368.
[22] F.L. Bleken, S. Chavan, U. Olsbye, M. Boltz, F. Ocampo, B. Louis, Appl. Catal., A 447–448 (2012) 178.
[23] J. Arichi, B. Louis, Cryst. Growth Des. 8 (2008) 3999.
[24] B. Louis, A. Vicente, C. Fernandez, V. Valtchev, J. Phys. Chem. C 115 (2011) 18603.
[25] B. Louis, S. Walspurger, J. Sommer, Catal. Lett. 93 (2004) 81.
[26] L.R. Aramburo, J. Ruiz-Martínez, L. Sommer, B. Arstad, R. Buitrago-Sierra, A. Sepúlveda-Escribano, H.W. Zandbergen, U. Olsbye, F.M.F. de Groot, B.M. Weckhuysen, ChemCatChem 5 (2013) 1386.